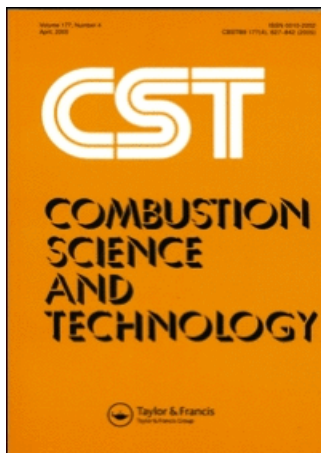


This article was downloaded by:[Cornell University Library]
On: 20 December 2007
Access Details: [subscription number 770490391]
Publisher: Taylor & Francis
Informa Ltd Registered in England and Wales Registered Number: 1072954
Registered office: Mortimer House, 37-41 Mortimer Street, London W1T 3JH, UK



Combustion Science and Technology

Publication details, including instructions for authors and subscription information:

<http://www.informaworld.com/smpp/title~content=t713456315>

Probability Calculations for Turbulent Jet Flows with Mixing and Reaction of NO and O₃

P. Givi^a; W. A. Sirignano^a; S. B. Pope^b

^a Department of Mechanical Engineering, Carnegie-Mellon University., Pittsburgh., PA 15213

^b Sibley School of Mechanical and Aerospace Engineering, Cornell University., Ithaca., NY 14853

Online Publication Date: 01 May 1984

To cite this Article: Givi, P., Sirignano, W. A. and Pope, S. B. (1984) 'Probability Calculations for Turbulent Jet Flows with Mixing and Reaction of NO and O₃',

Combustion Science and Technology, 37:1, 59 - 78

To link to this article: DOI: 10.1080/00102208408923746

URL: <http://dx.doi.org/10.1080/00102208408923746>

PLEASE SCROLL DOWN FOR ARTICLE

Full terms and conditions of use: <http://www.informaworld.com/terms-and-conditions-of-access.pdf>

This article maybe used for research, teaching and private study purposes. Any substantial or systematic reproduction, re-distribution, re-selling, loan or sub-licensing, systematic supply or distribution in any form to anyone is expressly forbidden.

The publisher does not give any warranty express or implied or make any representation that the contents will be complete or accurate or up to date. The accuracy of any instructions, formulae and drug doses should be independently verified with primary sources. The publisher shall not be liable for any loss, actions, claims, proceedings, demand or costs or damages whatsoever or howsoever caused arising directly or indirectly in connection with or arising out of the use of this material.

Probability Calculations for Turbulent Jet Flows with Mixing and Reaction of NO and O₃

P. GIVI and W. A. SIRIGNANO *Department of Mechanical Engineering,
Carnegie-Mellon University, Pittsburgh, PA 15213*

S. B. POPE *Sibley School of Mechanical and Aerospace Engineering,
Cornell University, Ithaca, NY 14853*

(Received April 15, 1983; in final form November 7, 1983)

Abstract—Calculations are performed for non-premixed, chemically reacting axisymmetric and plane jets involving NO and O₃. The jet carries NO diluted with N₂ into the stagnant surrounding containing traces of O₃ in the carrier gas N₂. The concentrations of the reactants and products are determined from Monte Carlo solutions of the joint PDF equation of two scalars (Shvab-Zeldovich variables). The hydrodynamics are determined from the continuity equation, time averaged momentum equations and a two-equation model for turbulence. In order to compare the Monte Carlo calculations and to estimate the effects of concentration fluctuations on the reaction rate, finite-difference calculations were made on the averaged transport equations for the same two Shvab-Zeldovich variables, with neglect of second-order effects on the reaction rate. It is noted that for the passive scalar (first Shvab-Zeldovich variable) mean transport calculations are advantageous, where the joint PDF formulation has the advantage of closing the source term for the reactive scalar (second Shvab-Zeldovich variable). This paper contains mean velocity profiles, turbulence scales, the mean and all the second-order moments of scalars calculated from joint PDF formulation.

1 INTRODUCTION

There is a continuing need to develop accurate theoretical tools to predict the behavior of turbulent chemically reacting flows. In order to achieve this goal, the use of a system which could give us a good physical understanding is important. The system used here is the non-premixed isothermal reaction of NO and O₃ diluted with N₂. This system has well known rate constants. The main reason for this choice is that any uncertainty in the kinetics calculations would inhibit the evaluation of the errors associated with our other turbulent-model assumptions. Note further that, while the PDF evolution equation employed in this paper contains a modeled representation of turbulent transport and of molecular mixing, the chemical kinetic representation is exact.

The flow field is determined from the continuity equation, the mean momentum equation, and the $k-\epsilon$ (Launder and Spalding, 1972) model of turbulence which determines the turbulent viscosity. The errors associated with this turbulence model have been reported (Ramos, 1980), but it has proven to be successful to some degree for both reacting shear flows (Parker and Sirignano, 1981), and wall-bounded elliptic type turbulent flows (Ramos *et al.*, 1981). For the cases considered here, this model seems to be satisfactory. The concentrations of the species involved can be determined from a model equation for the joint PDF of the two Shvab-Zeldovich variables. This kind of formulation does not need any model for the second-order moments. The concentration of the species could also be determined from the averaged transport equations of the same two Shvab-Zeldovich variables, but the

models for determinations of the scalar fluctuations are not very satisfactory. In a chemical reaction, these fluctuations tend to decrease the formation rate of the products. In order to estimate the effects of these fluctuations they were set to zero in the mean transport equations. A comparison between the mean concentration profiles of the products obtained from the averaged transport equation and the PDF formulation and also the profiles of these moments would give us some useful information about the importance of these fluctuations. A finite-difference method (Pope, 1977) was used for the solution of averaged transport equations of the flow and the concentration fields. The PDF equation was solved by a Monte Carlo method developed by Pope (1981).

In the next section, the flow field formulation and the treatment of the species concentrations are described. The results for both axisymmetric and plane jet calculations are presented in Section 3, where the summary and conclusions are given in Section 4.

2 FORMULATION

Hydrodynamic Field

Figure 1 shows the geometries considered in this study. The particular jet configuration was chosen to correspond to an experiment which is to be developed. All the equations in this section are presented in their nondimensional form. The coordinates in physical space, x and r (x and y in plane jet), are normalized to \mathcal{X} and η , such that

$$\mathcal{X} = \int \delta^{-1}(x) dx \quad (1)$$

$$\eta = \frac{y}{\delta(x)}, \quad 0 \leq \eta \leq 3.0 \text{ for jets}, \quad (2)$$

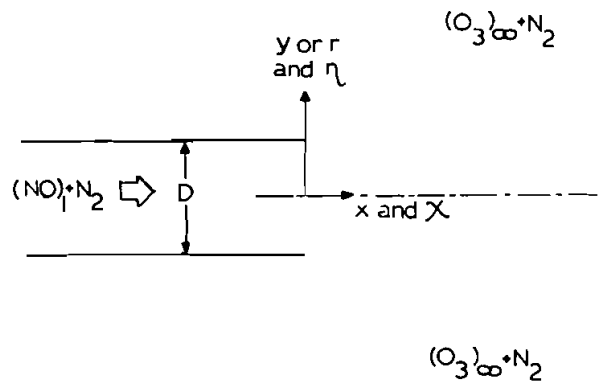


FIGURE 1 Geometry.

where $y \equiv r$ for cylindrical coordinates and $\delta(x)$ is the distance to the location where the velocity is half its center-line velocity. The mean velocity field is normalized by

$$U^*(X, \eta) = U(x, y)/U_0(x) \quad (3)$$

$$V^*(X, \eta) = \frac{V(x, y)}{U_0(x)} - U^*(X, \eta) \left(\eta \frac{d\delta}{dx} \right), \quad (4)$$

where $U_0(x)$ is the mean center-line velocity and obviously varies with x . The boundary-layer momentum equations were solved for axial velocity U , radial velocity V , kinetic energy k , and eddy dissipation ϵ . The turbulent viscosity is then determined from

$$\mu_t = C_\mu \rho k^2/\epsilon, \quad (5)$$

where $C_\mu = 0.09$.

Concentration Fields

The chemical reactions employed include the reaction of NO in the jet and O₃ in the surrounding flow (see Figure 1). The flow is diluted with N₂ to make the process isothermal and constant density. The flow is parabolic. The pressure, which is constant, is determined from

$$P = \rho RT \sum_j \frac{Y_j}{W_j} = \rho \frac{R}{W_{N_2}} T. \quad (6)$$

The reaction between the species is one-step and is assumed to be irreversible,



With the boundary-layer approximations, incompressible flow with constant properties and equal turbulent diffusion coefficients (*i.e.*, $\Gamma_{ij} = \Gamma_{jt} = \text{constant} = \Gamma$), neglect of the body forces, bulk viscosity, and use of Fick's law, the time-averaged transport equations are written as (Williams, 1965)

$$L(C_j) = U \frac{\partial C_j}{\partial x} + V \frac{\partial C_j}{\partial y} - \frac{1}{r} \frac{\partial}{\partial y} \left[r \Gamma \frac{\partial C_j}{\partial y} \right] = \langle \omega_j \rangle, \quad (8)$$

where $r \equiv 1$ for plane jet, and $y \equiv r$ for axisymmetric jet. C_j is the ensemble averaged value of concentration of species j ; ω_j is the rate of the reaction of species j , and is given by

$$\langle \omega_{NO} \rangle = \langle \omega_{O_3} \rangle = \langle -\omega_{O_2} \rangle = \langle -\omega_{NO_2} \rangle = -K_f C_{NO} C_{O_3} - K_f \langle c_{NO}' c_{O_3}' \rangle, \quad (9)$$

where c_j' is the fluctuation of the concentration of species j and

$$K_f = 9.28 \times 10^6 \frac{\text{m}^3}{\text{kgmole-sec}}. \quad (10)$$

Because of the linear dependence of the four species, they can be replaced by two Shvab-Zeldovich variables as follows

$$\left. \begin{aligned} \phi_1 &= [C_{NO} + C_{NO_2}]/[(C_{NO})_i] \quad \text{or} \\ \phi_1 &= [(C_{O_3})_\infty - (C_{O_3}) - (C_{NO_2})]/(C_{O_3})_\infty, \end{aligned} \right\} \quad (11)$$

which is a passive scalar, and a product concentration

$$\phi_2 = C_{\text{NO}_2}/(C_{\text{O}_3})_\infty \quad \text{or} \quad \phi_2 = C_{\text{O}_2}/(C_{\text{O}_3})_\infty. \quad (12)$$

Now we define

$$\left. \begin{aligned} \alpha &= (C_{\text{NO}})_l/(C_{\text{O}_3})_\infty \\ \beta &= (C_{\text{O}_3})_\infty/(C_{\text{N}_2})_\infty. \end{aligned} \right\} \quad (13)$$

In terms of α and β and with use of Eq. (6), we have

$$\left. \begin{aligned} L(\phi_1) &= 0 \\ L(\phi_2) &= \langle \omega(\phi_1, \phi_2) \rangle = \langle \beta\Omega(\alpha\phi_1 - \phi_2)(1 - \phi_1 - \phi_2) \rangle, \end{aligned} \right\} \quad (14)$$

where $\Omega = PK_f/RT = 4 \times 10^5 \text{ sec}^{-1}$ at atmospheric conditions. It is clearly seen from (12) and (13) that once ϕ_1 and ϕ_2 are determined, then the concentrations of all the species could be calculated. Neglecting the scalar fluctuations, we would have

$$\langle \omega(\phi_1, \phi_2) \rangle = \omega(\langle \phi_1 \rangle, \langle \phi_2 \rangle) = \beta\Omega(\alpha\langle \phi_1 \rangle - \langle \phi_2 \rangle)(1 - \langle \phi_1 \rangle - \langle \phi_2 \rangle). \quad (15)$$

Equations (14) and (15) could be cast into non-dimensional form by

$$\begin{aligned} \underline{r} &= r/\delta^* \text{ (axisymmetric)} \quad \text{or} \quad \underline{r} = 1 \text{ (plane)} \\ \text{and} \\ \delta^* &= \delta(x) \text{ (axisymmetric)} \quad \text{or} \quad \delta^* = 1 \text{ (plane)} \end{aligned}$$

$$\left. \begin{aligned} \mu^* &= \frac{\mu}{U_0\delta} \\ \Gamma^* &= \frac{\Gamma}{U_0\delta} = \frac{\mu^*}{SC_t}, \quad SC_t = 0.7. \end{aligned} \right\} \quad (16)$$

Then the equations become

$$L^*(\phi_1) = 0 \quad (17)$$

$$L^*(\phi_2) = \frac{\delta}{U_0} \beta\Omega(\alpha\langle \phi_1 \rangle - \langle \phi_2 \rangle)(1 - \langle \phi_1 \rangle - \langle \phi_2 \rangle) \quad (18)$$

$$L^* = U^* \frac{\partial}{\partial \chi} + V^* \frac{\partial}{\partial \eta} - \frac{1}{\underline{r}} \frac{\partial}{\partial \eta} \left(\underline{r} \Gamma^* \frac{\partial}{\partial \eta} \right). \quad (19)$$

The boundary conditions are

$$\begin{aligned} (\phi_1)_l = 1, \quad \frac{\partial(\phi_1)}{\partial \eta} \Big|_{\eta=0} &= 0 & \phi_1|_{\eta=3.0} &= 0.0 \\ (\phi_2)_l = 0, \quad \frac{\partial(\phi_2)}{\delta \eta} \Big|_{\eta=0} &= 0, & \phi_2|_{\eta=3.0} &= 0.0. \end{aligned} \quad (20)$$

Joint PDF Transport Equation

As mentioned before, all the information concerning the concentrations could be found from the solution of ϕ_1 and ϕ_2 . Therefore, the joint PDF of ϕ_1 and ϕ_2 [$p(\psi, X, \eta, t)$, $\psi = \psi_1, \psi_2$] would provide a complete statistical description of all the scalars. The PDF is defined so that $p(\psi_1, \psi_2)d\psi_1 d\psi_2$ is the probability of ϕ_1 and ϕ_2 in the range

$$\left. \begin{aligned} \psi_1 < \phi_1 < \psi_1 + d\psi_1 \\ \psi_2 < \phi_2 < \psi_2 + d\psi_2. \end{aligned} \right\} \quad (21)$$

The normalized modeled transport equation for the joint PDF of scalars for two-dimensional boundary layer flow is as follows (Pope, 1979):

$$U^* \frac{\partial p}{\partial x} + V^* \frac{\partial p}{\partial \eta} - \frac{1}{r} \frac{\partial}{\partial \eta} \left(r \Gamma^* \frac{\partial p}{\partial \eta} \right) = \frac{\partial}{\partial \psi_2} \left[\frac{\delta p}{U_0} \omega(\psi_1, \psi_2) \right] + \Omega_T^* E(\psi_1, \psi_2), \quad (22)$$

where the last term on the right-hand side describes the molecular mixing term. There are some models for this term (e.g., Pope, 1976; Dopazo, 1975) which are not entirely satisfactory. Employing Curl's model (Curl, 1963) for this term, we have

$$\begin{aligned} E(\psi_1, \psi_2) = 4 \int \int p(\psi_1 + \psi_1^*, \psi_2 + \psi_2^*) \\ \times p(\psi_1 - \psi_1^*, \psi_2 - \psi_2^*) d\psi_1^* d\psi_2^* - p(\psi_1, \psi_2). \end{aligned} \quad (23)$$

It is assumed that the Reynolds number is so high that the rate of molecular mixing is given by the lowest turbulence frequency:

$$\Omega_T = 2C\phi \frac{\varepsilon}{k}, \quad C\phi = 2.0 \quad (24)$$

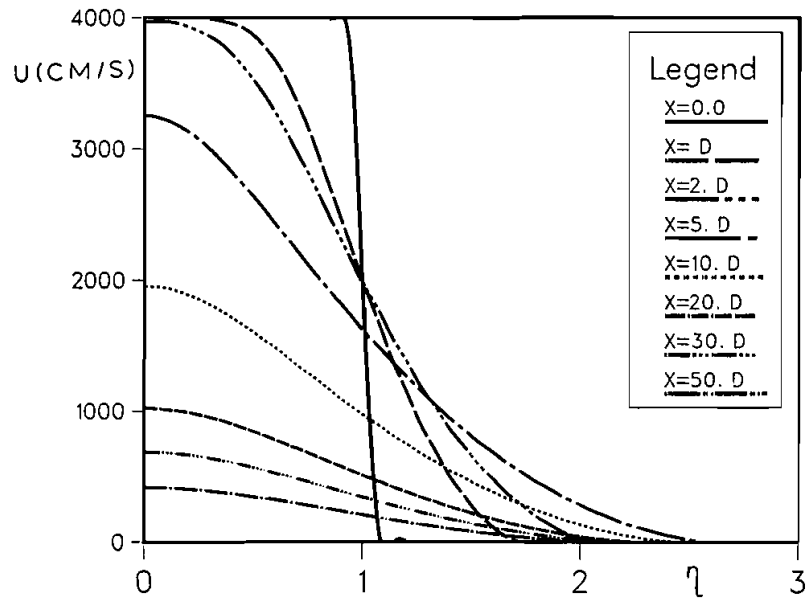
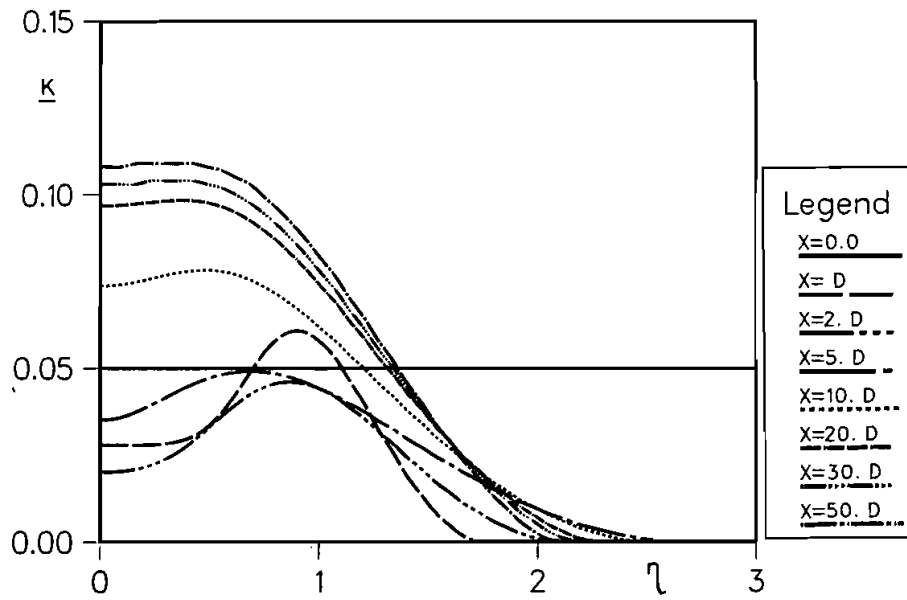
and in non-dimensional form

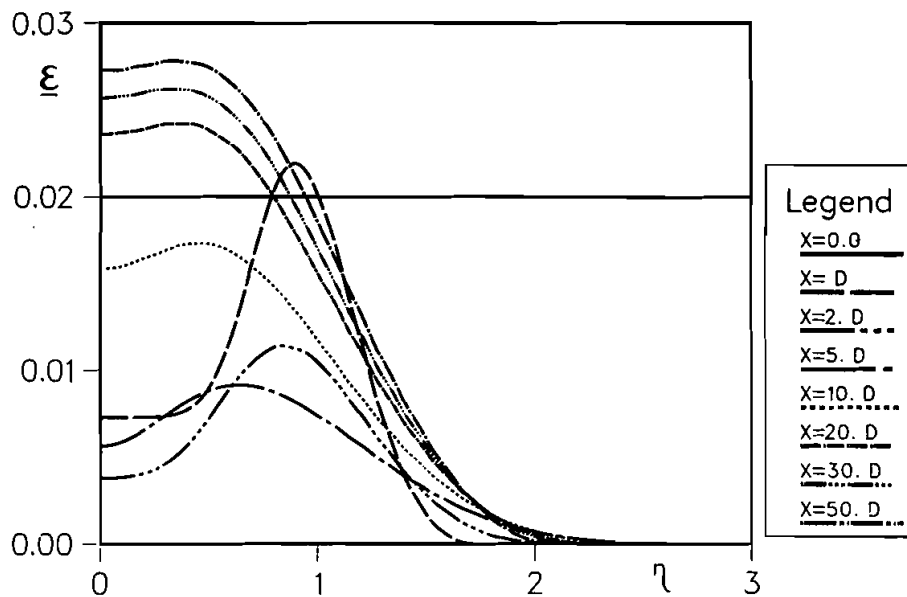
$$\Omega_T^* = \Omega_T \frac{\delta}{U_0}. \quad (25)$$

This model for molecular mixing seems to be satisfactory, because of its applicability to any number of scalars.

3 PRESENTATION OF RESULTS

The modeled PDF equation and mean transport equations were solved for $0 \leq x \leq 50D$, where D is the diameter in the axisymmetric case and the distance between the two plates in plane jet calculations. There were 48 finite-difference nodes across the flow and the PDF was represented by an ensemble of 600 elements at each nodal point. Some of the calculations were repeated with 100 grid nodes to check that the truncation error was insignificant. The initial value of the velocity was set to 40 m/sec uniformly across the jet exit. The value of D was set to 4 cm, to make the Reynolds number to be 1.6×10^5 at the exit. The initial values of $\underline{k} = k/[U_0(x)]^2$ and $\underline{\varepsilon} = \varepsilon\delta(x)/[U_0(x)]^3$ were set to 0.05 and 0.02, respectively. The concentrations of

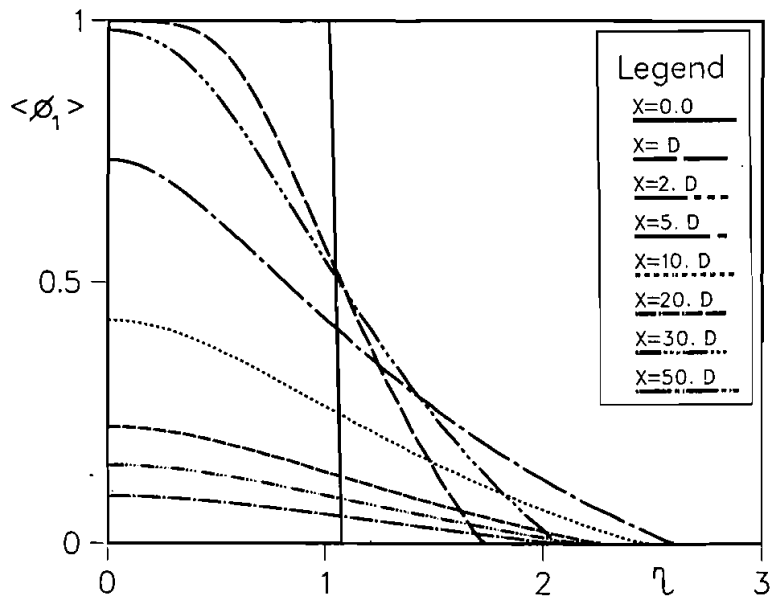
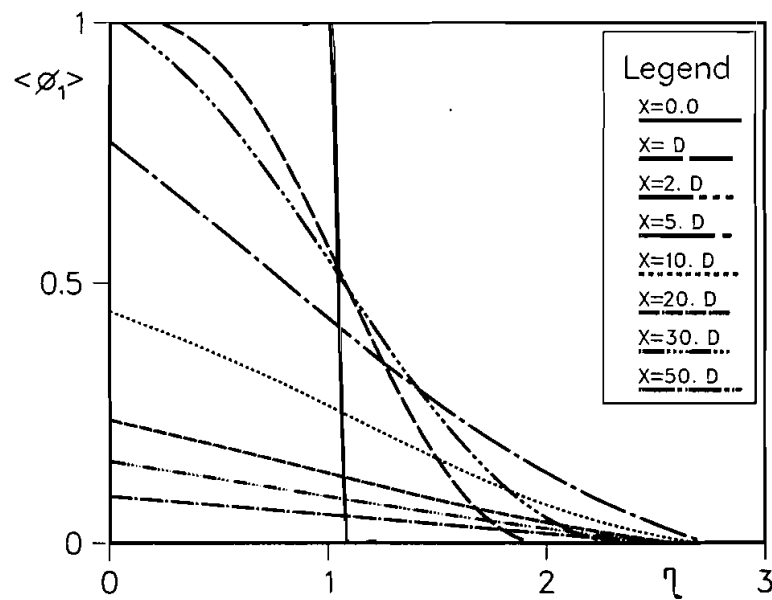
FIGURE 2 Axisymmetric jet. U -velocity (cm/sec) vs. η .FIGURE 3 Axisymmetric jet. k vs. η .

FIGURE 4 Axisymmetric jet. $\underline{\epsilon}$ vs. η .

O_3 and NO were set to 0.1 and 0.2 percent, respectively. This would make $\alpha=2.0$ and $\beta\Omega=400$. The marching step in the x direction (Δx) was chosen to be very small, $\Delta x=0.025\delta(x)$, thus eliminating the source of truncation error. Some calculations with smaller Δx were repeated to check the insignificance of the truncation error. The results of the calculations for both cases are discussed separately.

Axisymmetric Jet Results

Figures 2, 3 and 4 represent the flow field profile. Although the $k-\epsilon$ model of turbulence is well known not to predict the axisymmetric flows very well, it is qualitatively acceptable for our purpose. That is, we expect that our major conclusions are not dependent on the quantitative accuracy of the model. Figures 5 and 6 show the $\langle\phi_1\rangle$ profile calculated from mean transport equation and joint PDF calculations, respectively. From these figures it is seen that the results are very close and the only differences between the two figures are due to the different numerical procedures involved. The profile of $\langle\phi_2\rangle$ calculated from the mean transport equation with neglect of second-order moments is shown in Figure 7, where the smoothed profile of $\langle\phi_2\rangle$ from joint PDF formulation is represented by Figure 8. It is clear from these two figures that the finite-difference calculation of the mean transport equation predicts higher products formation and that it is simply due to neglect of the second-order fluctuations. These second-order moments tend to decrease the value of the source term in Eq. (14) resulting in decrease of the products. These two figures show the dependence of the product formations on the local Damköhler number $\{Da=(\beta\Omega)/[U_0(x)/\delta(x)]\}$. The value of Da at the jet exit is 0.2 and it increases to about 0.93 at $x=10D$. In the region of small $Da(Da \ll 1, 0 \leq x \leq 5D)$ we can see

FIGURE 5 Axisymmetric jet. $\langle \phi_1 \rangle$ vs. η . Mean conservation equation.FIGURE 6 Axisymmetric jet. $\langle \phi_1 \rangle$ vs. η . Joint PDF equation.

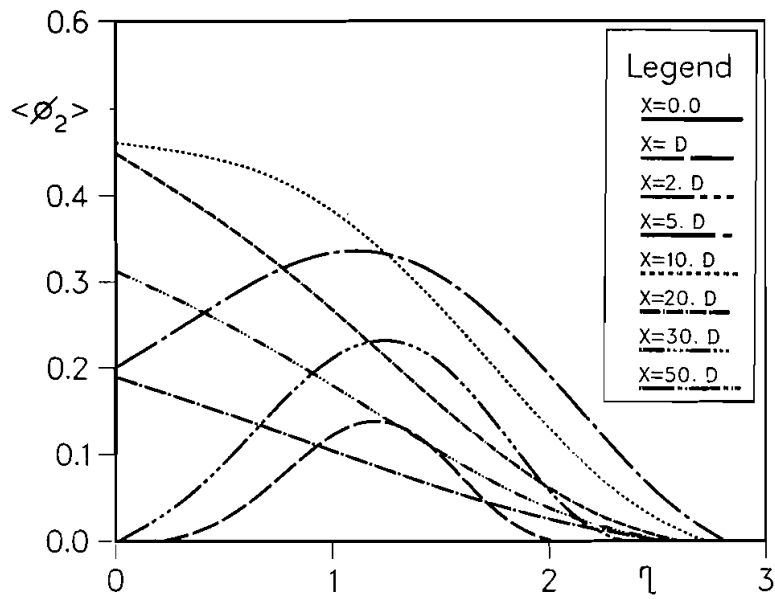


FIGURE 7 Axisymmetric jet. $\langle \phi_2 \rangle$ vs. η . Mean reaction rate model.

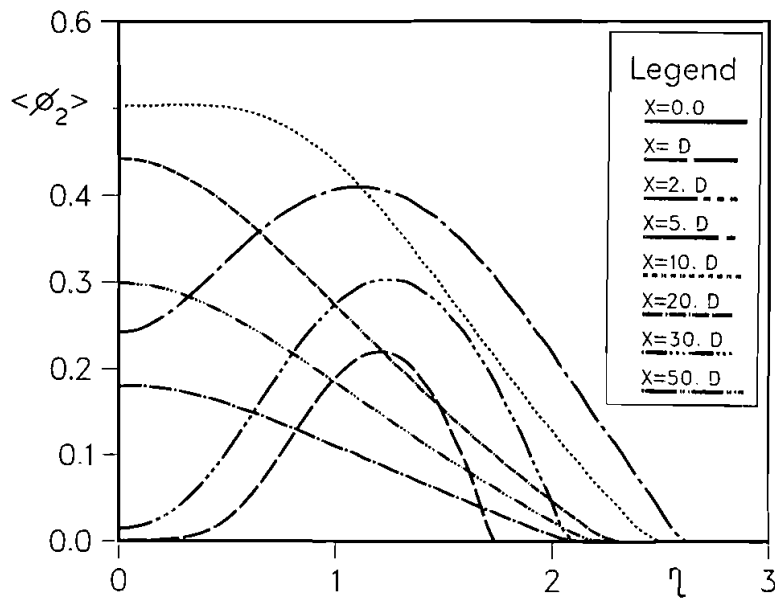


FIGURE 8 Axisymmetric jet. $\langle \phi_2 \rangle$ vs. η . Joint PDF model.

that little reaction occurs and therefore a small amount of product is formed. It should be noted that the Damköhler number as chosen is not the relevant choice for the first few diameters of length. That is, in the initial region where a core flow surrounded by a mixing layer exists, the mixing layer thickness rather than jet diameter is the correct length to employ in the calculation of a Damköhler. However, such a calculation would only make the Damköhler number smaller in the initial region and not change any of the conclusions. On the other hand, in the region where x is greater than $30D$ ($Da=7.19 \gg 1$) $\langle \phi_2 \rangle$ adopts its equilibrium value and after this point it diffuses to small values, and no more reaction appears. In the intermediate region ($Da \sim 1.0$, $x \sim 10D$) it is clear from these figures that reaction proceeds at a rate similar to the order of the turbulence frequency Ω_T . In other regions where the Damköhler number is not very much greater than 1, the reaction is diffusion limited and also proceeds at a rate close to the turbulence frequency. As mentioned before, the only difference between these two profiles is due to the presence of the second-order moments, which are shown in Figures 9–11. The profile of $\langle \phi_1' \phi_1' \rangle$ rises to some maximum and then decreases with increase in η . It diffuses more and more in η direction as we move along x until it tends to zero further downstream, as one might expect. The profile of $\langle \phi_2' \phi_2' \rangle$ is shown in Figure 10. A comparison between Figures 9 and 10 shows the difference between the fluctuations of the conserved and the reactive scalar. Comparing Figures 10 and 8 shows that the maximum of $\langle \phi_2' \phi_2' \rangle$ is at the same place as the largest $\langle \phi_2 \rangle$ gradient. This effect can be explained by the fact that the fluctuations would be greatest at the point of maximum gradient. The profiles of $\langle \phi_1' \phi_2' \rangle$ are zero at the jet boundary and before $x=10D$ all of these profiles decrease monotonically to negative minimum values and then monotonically increase to their positive maximum values and decrease monotonically again to zero. Before $x=10D$ all of these profiles pass through the zero point at $1 \leq \eta \leq 1.2$. After $x=20D$ they have positive values throughout the range of η .

To examine the effects of these fluctuations more, Figure 12 is presented. This figure shows the profiles of $\langle \phi_2 \rangle$, solved from the mean transport equation of $\langle \phi_2 \rangle$ where all the second order moments calculated from Monte Carlo solution of the joint PDF formulation are substituted back in the source term in Eq. (14). From this figure it is clear that the mass flow rate of the product predicted by this model is less than that of the other two methods for Damköhler number greater than $0.93(x \geq 10D)$; however, for Damköhler numbers less than this value the amount of mass flow rate predicted by this model is between the other two models. This model is essentially a second-order closure model where all the moments are calculated from the joint PDF calculations. The differences between this model and Monte Carlo calculations are basically due to different numerical methods involved.

The Curl model of molecular mixing is well known to present some unrealistic behavior in the details of the PDF, in particular various delta functions tend to be created. While some trust can be placed in the representation of the mean quantities and moments derived from the PDF, little value is seen in displaying the joint PDF graphically for either the axisymmetric or the planar case.

Plane Jet Results

The $k-\epsilon$ model of turbulence predicts the flow profile as shown by Figures 13, 14 and 15. Comparing Figures 3 and 14 shows that the kinetic energy of turbulence is generally higher for axisymmetric flows. Comparison of Figures 4 and 15 also shows the higher rate of dissipation for the axisymmetric flows. Figures 16 and 17

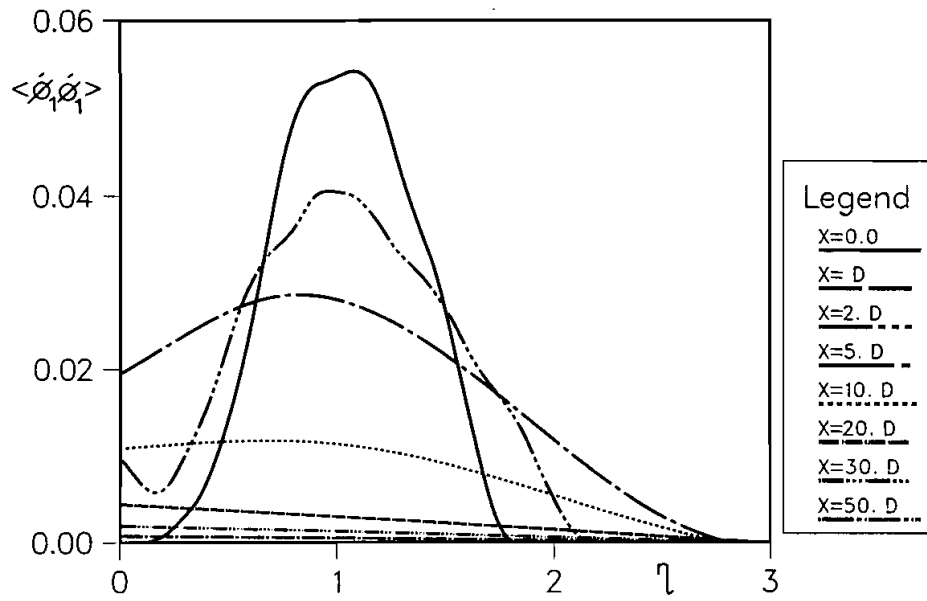


FIGURE 9 Axisymmetric jet. $\langle \phi_1' \phi_1' \rangle$ vs. η . Joint PDF model.

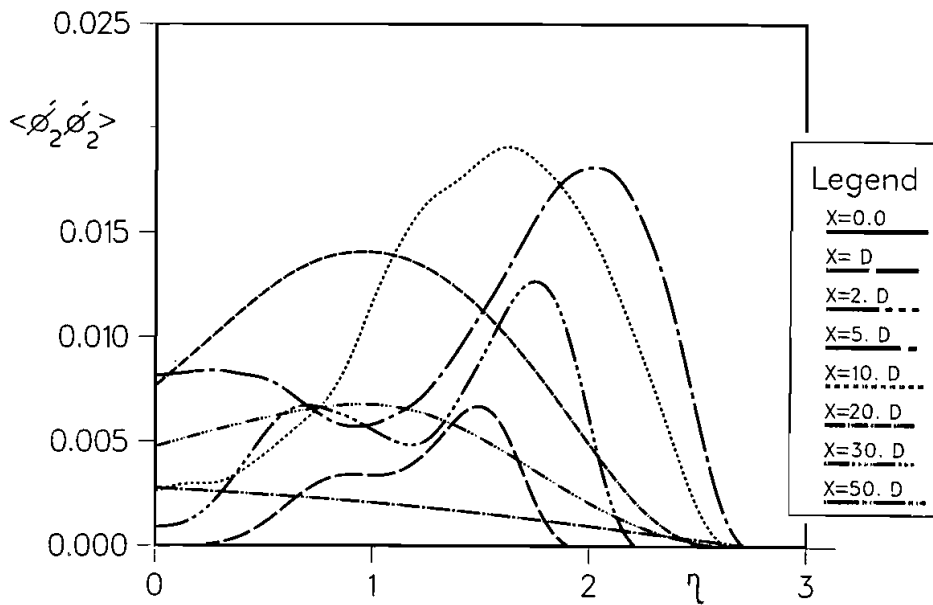


FIGURE 10 Axisymmetric jet. $\langle \phi_2' \phi_2' \rangle$ vs. η . Joint PDF model.

D

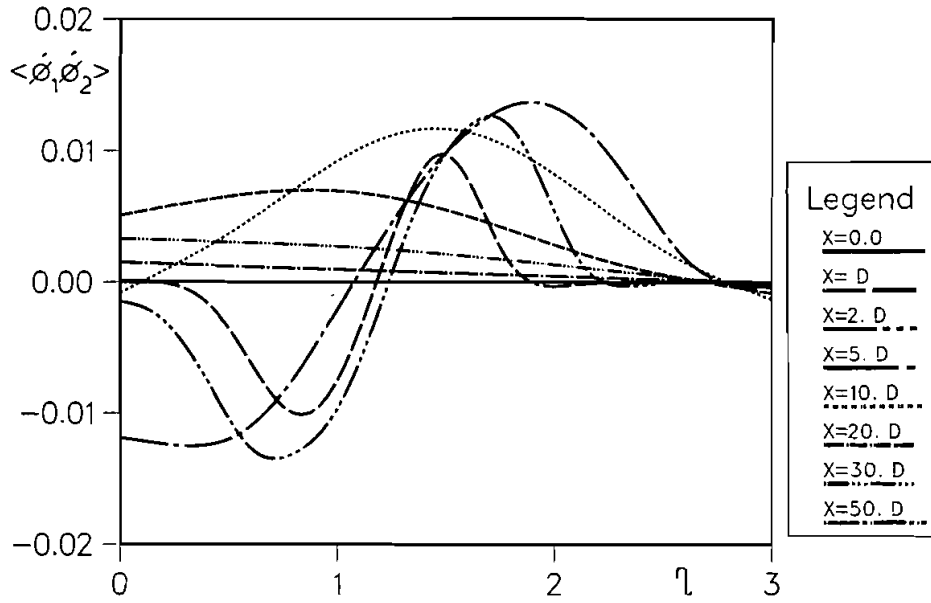


FIGURE 11 Axisymmetric jet. $\langle \phi_1' \phi_2' \rangle$ vs. η . Joint PDF model.

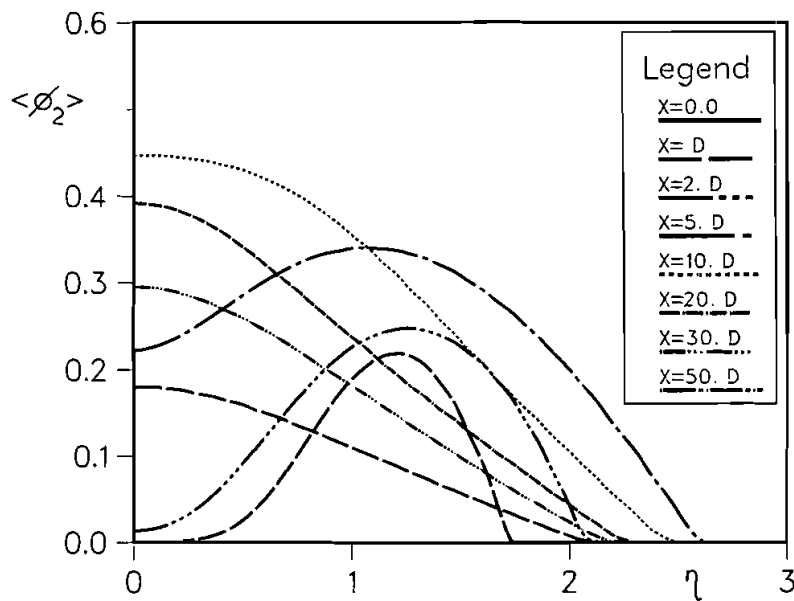


FIGURE 12 Axisymmetric jet. $\langle \phi_2 \rangle$ vs. η . Corrected reaction rate.

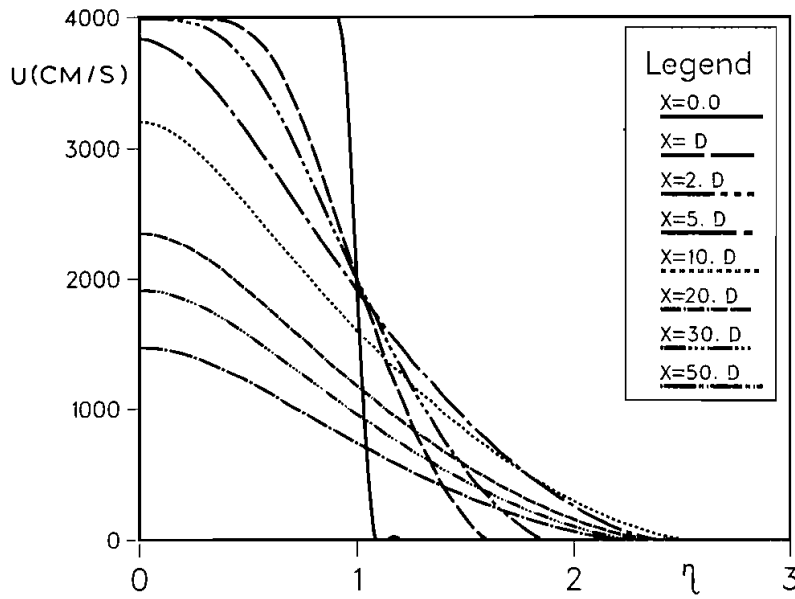


FIGURE 13 Plane jet. U -velocity (cm/sec) vs. η .

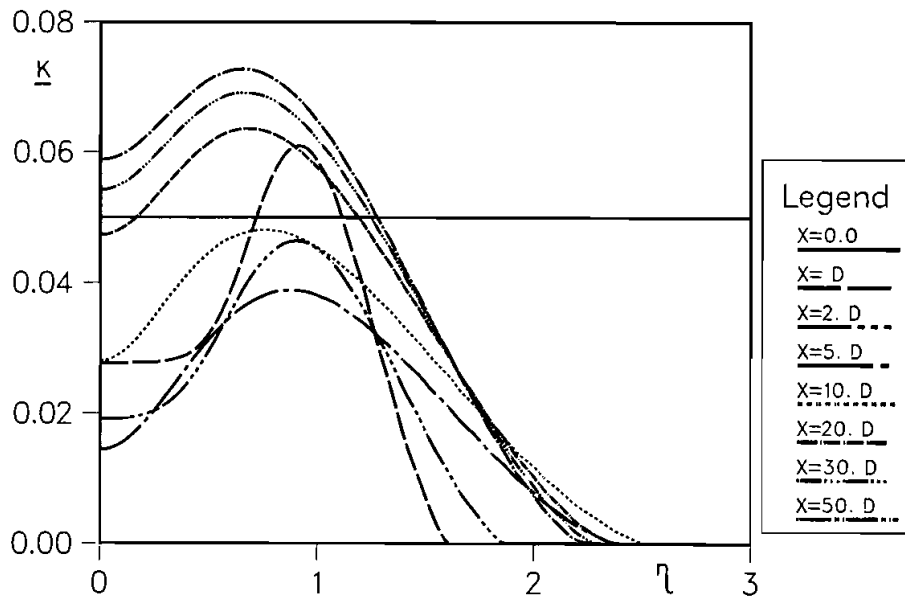
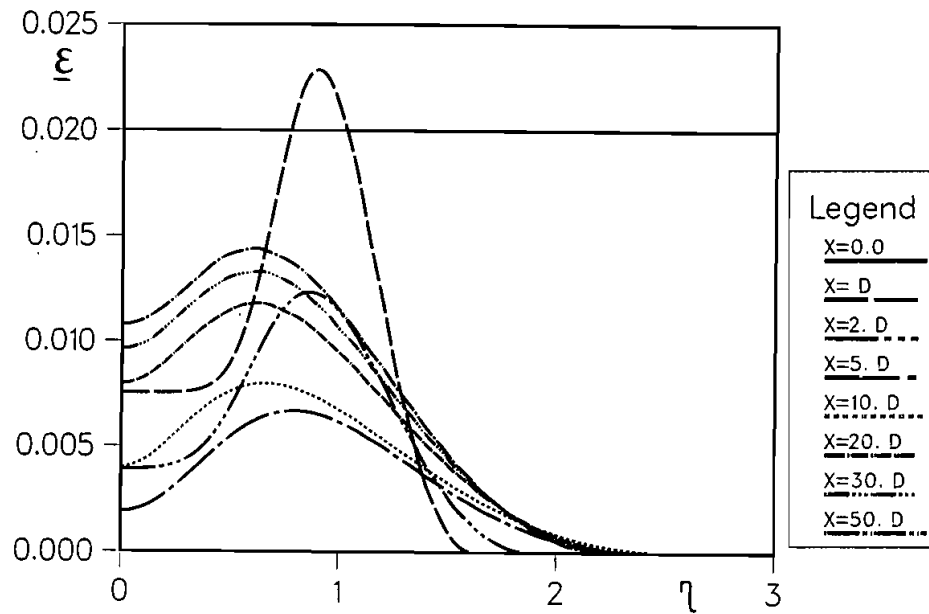
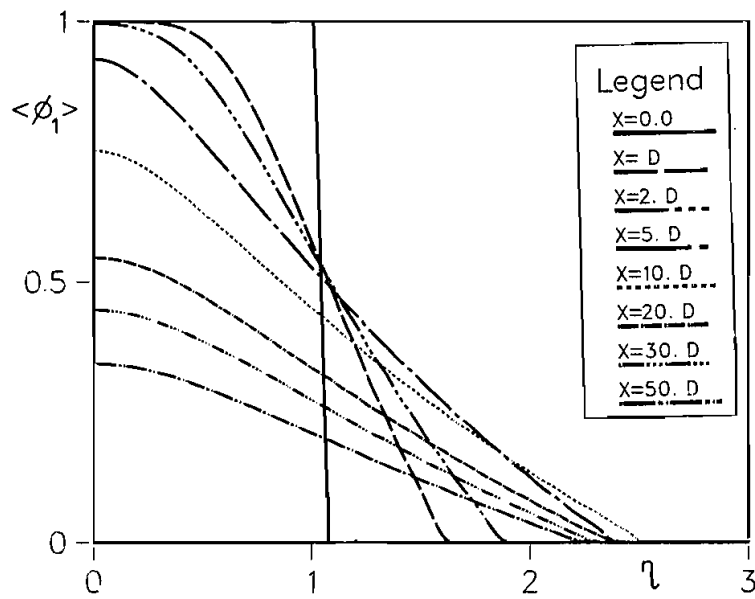


FIGURE 14 Plane jet. k vs. η .

FIGURE 15 Plane jet. $\underline{\epsilon}$ vs. η .FIGURE 16 Plane jet. $\langle \phi_1 \rangle$ vs. η . Mean conservation equation.

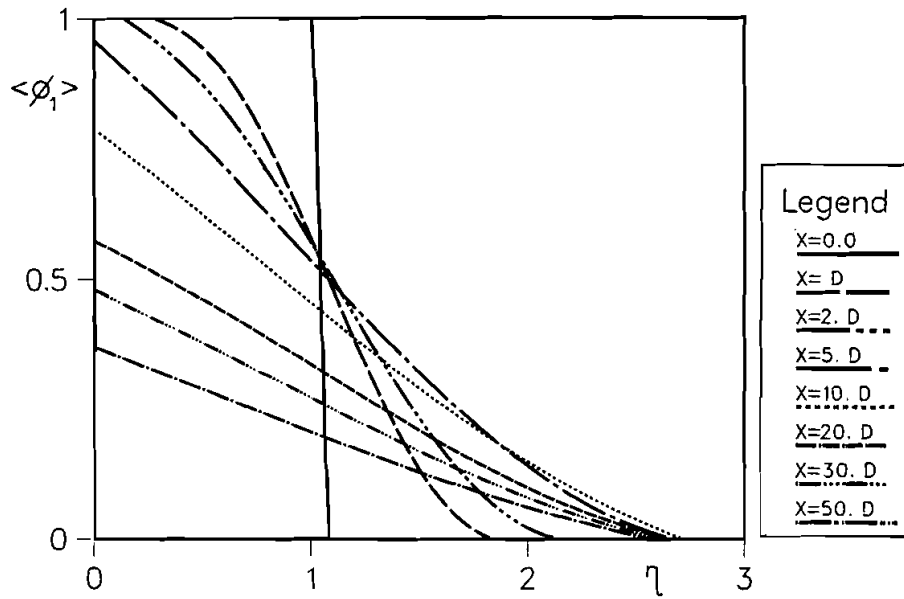


FIGURE 17 Plane jet. $\langle \phi_1 \rangle$ vs. η . Joint PDF equation.

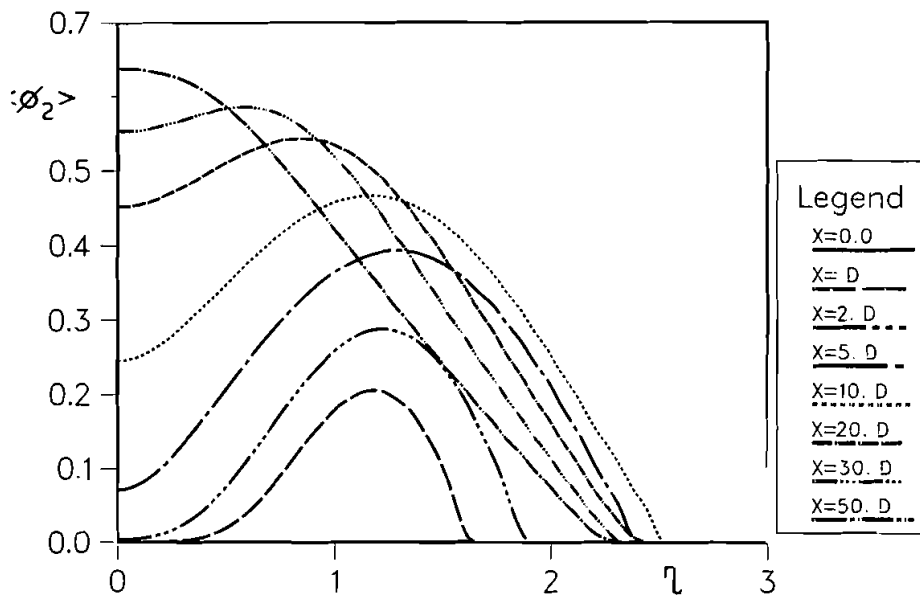
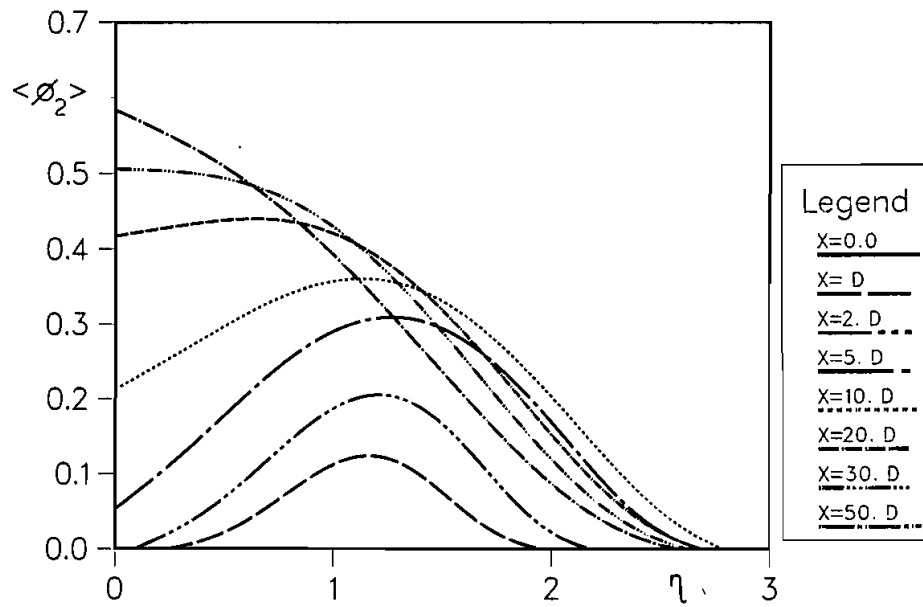
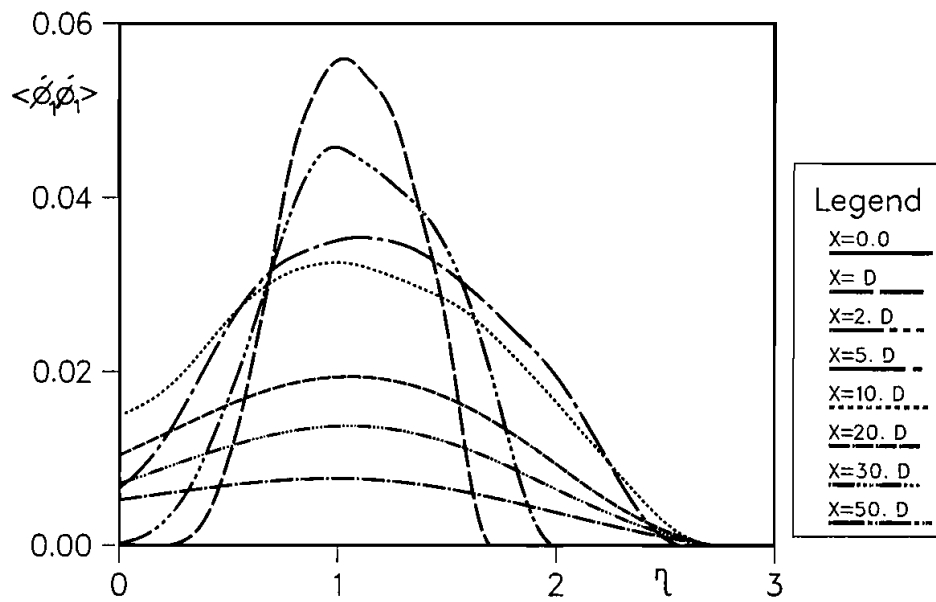


FIGURE 18 Plane jet. $\langle \phi_2 \rangle$ vs. η . Mean reaction rate model.

FIGURE 19 Plane jet. $\langle \phi_2 \rangle$ vs. η . Joint PDF model.FIGURE 20 Plane jet. $\langle \phi_1' \phi_1' \rangle$ vs. η . Joint PDF model.

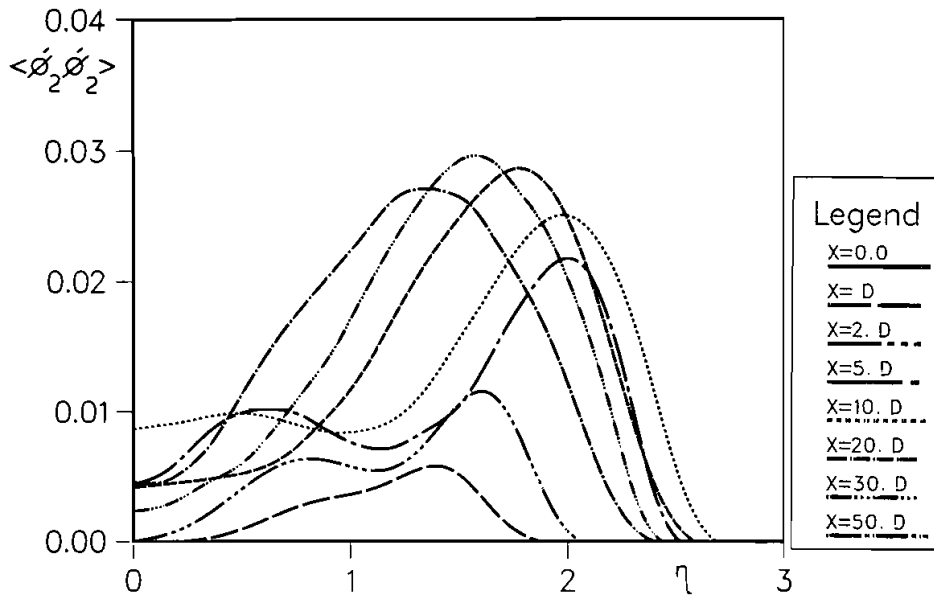


FIGURE 21 Plane jet. $\langle \phi_2' \phi_2' \rangle$ vs. η . Joint PDF model.

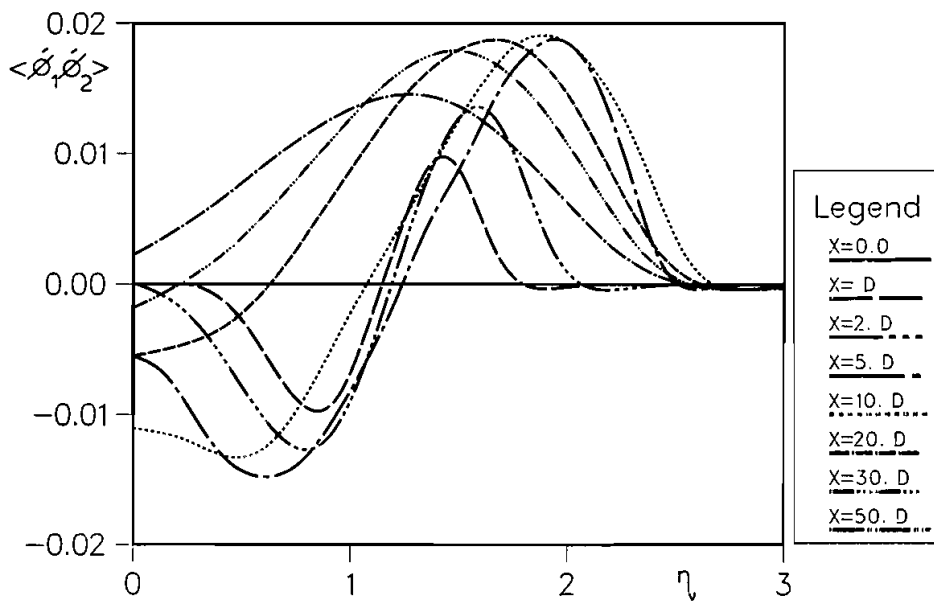


FIGURE 22 Plane jet. $\langle \phi_1' \phi_2' \rangle$ vs. η . Joint PDF model.

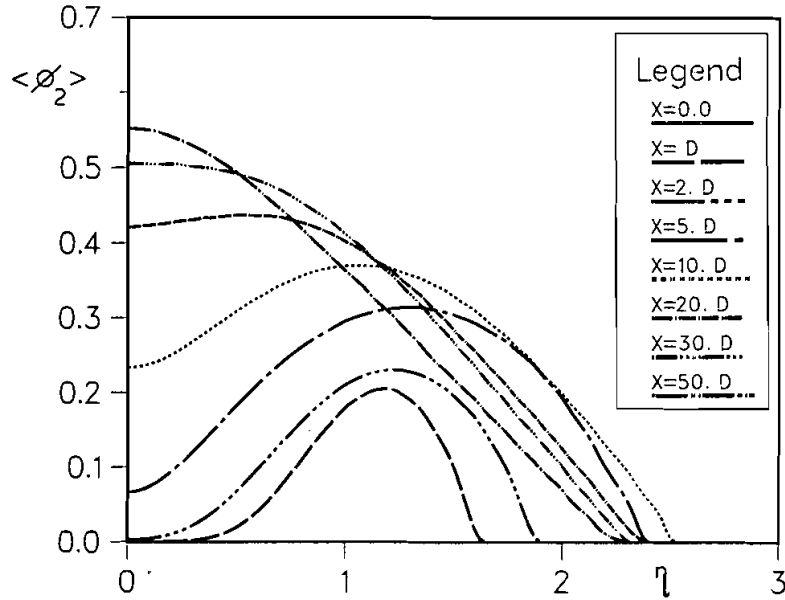


FIGURE 23 Plane jet. $\langle \phi_2 \rangle$ vs. η . Corrected reaction rate.

show the $\langle \phi_1 \rangle$ profile calculated from mean transport and joint PDF equation respectively. Their slight differences are again due to different numerical solution procedures. $\langle \phi_2 \rangle$ profile calculated from both methods is presented by Figures 18 and 19. Again the mean transport equation predicts higher product formation. It is clear from these two figures that after $50D$, $\langle \phi_2 \rangle$ has not yet adopted its equilibrium value ($Da=4.99$ at $x=50D$) and the reaction is, to some level, proceeding at a rate similar to turbulence frequency. For complete reaction, we still have to go more than $50D$. Second-order moments for plane jet are shown in Figures 20–22. The $\langle \phi_1' \phi_1' \rangle$ profile has the same trend as axisymmetric case. The $\langle \phi_2' \phi_2' \rangle$ has a slightly higher value for plane jet calculations. From Figure 21 it is clear that after $50D$ this value is still significant and is not diffusion limited. The $\langle \phi_1' \phi_2' \rangle$ profile for this case is shown in Figure 21. The general trend is as before. Before $x=10D$, all the profiles go monotonically to their negative minimum and then monotonically they increase to their positive maximum and then monotonically decrease to zero. After $x=10D$, all the profiles go to zero at $1 \leq \eta \leq 1.2$. Again, all of these moments calculated from joint PDF formulation are substituted back in the source term of the mean transport equation. The resulting profile of the product is presented in Figure 23. It is shown from this figure that the mass flow rate of product obtained by this model is less than the other two for Damköhler numbers greater than 1.2 ($x \geq 10D$) and the amount of the mass flow rate predicted by this model for Damköhler numbers less than 1 is between those obtained from the other two models.

4 SUMMARY AND CONCLUSIONS

Calculations have been presented for plane and axisymmetric turbulent jets involving the reaction between NO and O₃. The flow field is calculated from the boundary layer equations in conjunction with the k - ϵ turbulence model. The species concentrations are calculated from two different models. In the first model, the mean species concentration equations are solved by a finite-difference technique, and the effect of turbulent fluctuations on the reaction rate is ignored. In the second model, a transport equation for the joint PDF of the species is solved by a Monte Carlo method.

The calculations reported show that the neglect of species fluctuations in the mean-flow closure leads to a significant underestimation of the mean reaction rate. Thus, the PDF transport equation is advantageous in that it accounts exactly for the effect of species fluctuations on the mean reaction rate. The extension of the mean closure to include the effects of fluctuations is possible by adding modeled equations for the second moments. But these equations involve unknown third moments. Curl's model for molecular mixing is chosen because of its applicability to any number of scalars involved and it seems to be satisfactory to some degree. However, it only involves integral turbulent time scales, and models which account for finer turbulence time scales should be sought to represent this term.

Measurements of mean and fluctuating species concentrations in these reacting flows would be of great value. They would enable a quantitative assessment of the models to be made.

NOMENCLATURE

C_j	concentration of the species j (mean value)
c_j'	fluctuation of concentration of the species j
Da	Damköhler number
l	jet exit
k	turbulent kinetic energy
P	pressure
p	probability density function
R	universal gas constant
SC_t	turbulent Schmidt number
T	temperature
U, V	axial and radial velocity components
W_j	molecular weight of species j
x, y, r	coordinates
Y_j	mass fraction of species j

Greek Symbols

ρ	density
χ, η	non-dimensional coordinates
ϵ	eddy dissipation
ω_j	rate of production of species j by chemical reaction
ϕ_1, ϕ_2	Shvab-Zeldovich variables (scalar quantities)
ψ_1, ψ_2	scalar space

μ_t turbulent viscosity
 Γ' turbulent diffusion coefficient
 $\langle \rangle$ ensemble average

REFERENCES

- Curl, R. L. (1963). Dispersed phase mixing: I. Theory and effects of simple reactors. *AIChE J.* **9**, 175.
- Dopazo, C. (1975). Probability density function approach for a turbulent axisymmetric heated jet: center-line evolution. *Phys. Fluids* **18**, 397.
- Launder, B. E., and Spalding, D. B. (1972). *Lectures in Mathematical Models of Turbulence*, Academic Press.
- Parker, S. F., and Sirignano, W. A. (1981). Comparison among various theories for turbulent reacting, and planar mixing layers. In *Combustion in Reactive Systems. Progress in Aeronautics and Astronautics*, Bowen, J. R., Manson, N., Oppenheim, A. K., and Soloukhin, R. I. (Eds.), AIAA, **76**, 211.
- Pope, S. B. (1976). The probability approach to the modeling of turbulent reacting flows. *Combustion and Flame* **27**, 299.
- Pope, S. B. (1977). A novel calculation procedure for free shear flows. Imperial College Report FS/77/7.
- Pope, S. B. (1979). The statistical theory of turbulent flames. *Philos. Trans. Royal Soc. London* **291**, 529.
- Pope, S. B. (1981). A Monte Carlo method for the PDF equations of turbulent reactive flow. *Combustion Science and Technology* **25**, 159.
- Ramos, J. I. (1980). The k/ϵ model of turbulence in the limiting case $Re \rightarrow \infty$. Report CO/80/3, Department of Mechanical Engineering, Carnegie-Mellon University, Pittsburgh, PA.
- Ramos, J. I., Gany, A., and Sirignano, W. A. (1981). A theoretical-experimental study of turbulent flow field in a four-stroke, motored, I.C. engine. *AIAA Journal* **19**, 595.
- Williams, F. A. (1965). *Combustion Theory*, Addison-Wesley Publishing Company, Inc.